Acta Pharmaceutica Sinica B 2017;7(2):208–214

Chinese Pharmaceutical Association
Institute of Materia Medica, Chinese Academy of Medical Sciences

Acta Pharmaceutica Sinica B

www.elsevier.com/locate/apsb
www.sciencedirect.com

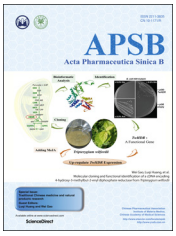

ORIGINAL ARTICLE

Molecular cloning and functional identification of a cDNA encoding 4-hydroxy-3-methylbut-2-enyl diphosphate reductase from *Tripterygium wilfordii*

Qiqing Cheng[a,b,c], Yuru Tong[a,b], Zihao Wang[a], Ping Su[a,b], Wei Gao[a,*], Luqi Huang[b,*]

[a]*School of Traditional Chinese Medicine, Capital Medical University, Beijing 100069, China*
[b]*National Resource Center for Chinese Materia Medica, Academy of Chinese Medical Sciences, Beijing 100700, China*
[c]*State Key Laboratory of Quality Research in Chinese Medicines, Macau University of Science and Technology, Macau, China*

Received 13 September 2016; revised 20 November 2016; accepted 12 December 2016

KEY WORDS

Tripterygium wilfordii;
Triptolide;
4-Hydroxy-3-methylbut-2-enyl diphosphate reductase;
Complementation;
Gene expression

Abstract The 4-hydroxy-3-methylbut-2-enyl diphosphate reductase (HDR) is the last step key enzyme of the methylerythritol phosphate (MEP) pathway, synthesizing isopentenyl diphosphate and its allyl isomer dimethylallyl diphosphate, which is important for regulation of isoprenoid biosynthesis. Here the full-length cDNA of *HDR*, designated *TwHDR* (GenBank Accession No. KJ933412.1), was isolated from *Tripterygium wilfordii* for the first time. TwHDR has an open reading frame (ORF) of 1386 bp encoding 461 amino acids. TwHDR exhibits high homology with HDRs of other plants, with an N-terminal conserved domain and three conserved cysteine residues. *TwHDR* cDNA was cloned into an expression vector and transformed into an *Escherichia coli hdr* mutant. Since loss-of-function *E.coli hdr* mutant is lethal, the result showed that transformation of *TwHDR* cDNA rescued the *E.coli hdr* mutant. This complementation assay suggests that the *TwHDR* cDNA encodes a functional HDR enzyme. The expression of *TwHDR* was induced by methyl-jasmonate (MJ) in *T. wilfordii* suspension cells. The expression of *TwHDR* reached the highest level after 1 h of MJ treatment. These results indicate that we have identified a functional TwHDR enzyme, which may play a pivotal role in the biosynthesis of diterpenoid triptolide in *T. wilfordii*.

*Corresponding author. Tel.: +86 10 83911671; Fex: +86 10 83911627 (Wei Gao).
E-mail addresses: weigao@ccmu.edu.cn (Wei Gao), huangluqi01@126.com (Luqi Huang).

Peer review under responsibility of Institute of Materia Medica, Chinese Academy of Medical Sciences and Chinese Pharmaceutical Association.

http://dx.doi.org/10.1016/j.apsb.2016.12.002

1. Introduction

Tripterygium wilfordii Hook. F., also known as Lei Gong Teng or thunder god vine, is native to eastern and southern China[1]. This vine-like plant belongs to the Celastraceae family, and has a long history of use in traditional Chinese medicine when treating autoimmune diseases and inflammatory dermatoses, such as psoriasis[2], erythema nodosum[3], rheumatoid arthritis[4], and systemic lupus erythematosus[5]. The research for the medicinal value of *T. wilfordii* has found out that the plant possesses anti-HIV, anti-inflammatory, antitumor, and anti-Parkinsonian effects[6–9], which arouses great interest in the field of medicine. The major active compound responsible for its medicinal functions is believed to be triptolide. Currently, only limited information on the biosynthesis of triptolide is available.

Triptolide is a diterpenoid triepoxide derived from isopentenyl diphosphate (IPP) and its isomer dimethylallyl diphosphate (DMAPP)[10]. There are two independent pathways leading to the biosynthesis of both IPP and DMAPP localized in different cellular compartments which are the cytosolic mevalonic acid (MVA) pathway and the plastidic 2-*C*-methyl-D-erythritol 4-phosphate (MEP) pathway[11,12]. While the MVA pathway is responsible for synthesizing sesquiterpenes and triterpenes, the MEP pathway is in charge of the biosynthesis of monoterpenes, diterpenes, and tetraterpenes[13]. As the last enzyme in the MEP pathway for isoprenoid biosynthesis, 4-hydroxy-3- methylbut-2-enyl diphosphate reductase (HDR) catalyzes (*E*)-4-hydroxy-3-methylbut-2-enyl diphosphate (HMBPP) into a mixture of 5:1 IPP and DMAPP (Fig. 1). Silencing of *HDR* gene in *Nicotiana benthamiana* can make the isoprenoid-derived chlorophyll and carotenoid pigments decrease to less than 4% of the control plants[14]. And overexpression of *HDR* gene contributes to increasing the production of isoprenoid-derived carotenoid and over-producing taxadiene up to 13-fold of the control group in transgenic *Arabidopsis*, proving its vital role in metabolic regulation of plastidial isoprenoid biosynthesis[15].

Because of the high toxicity, obtaining the effective components from *T. wilfordii* by traditional chemical methods is difficult spending much time and labor. And now the current studies regarding key enzymes of triptolide biosynthesis in *T. wilfordii* are few, and the production of triptolide still cannot be synthesized through biosynthesis methods. Based on the above issues, we present the cloning of full-length *HDR* cDNA of *T. wilfordii* (*TwHDR*) for the first time, proving it having the function of IspH and may acting a role as a potential key enzyme for the biosynthesis of triptolide.

2. Materials and methods

2.1. Plant material

T. wilfordii cell suspensions were cultured in Murashige and Skoog (MS) medium containing 30 g/L sucrose and 8 g/L agar with 0.5 mg/L 2,4-dichlorophenoxyacetic acid (2,4-D), 0.1 mg/L kinetin (KT), and 0.5 mg/L indole-3-butytric acid (IBA). All suspension cell cultures were maintained at 25 ± 1 °C with shaking by orbital shaker (DZ-100, Suzhou experimental equipment Co., Ltd., Suzhou, China) at 120 rpm in the dark.

2.2. RNA isolation

The 10-day-old *T. wilfordii* suspension cells were treated with MJ for 0, 1, 4, 12, 24, 48 and 72 h at a final concentration of 50 μmol/L.

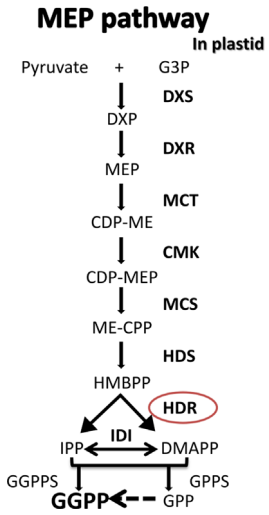

Figure 1 Schematic MEP pathway for GGPP. Multiple steps are indicated with striped arrows. G3P, glyceraldehyde 3-P; DXP, deoxyxylulose 5-P; MEP, methylerythritol 4-P; CDP-ME, 4-diphosphocytidyl-methylerythritol; CDP-MEP, CDP-ME 2-P; ME-CPP, methylerythritol 2,4-cyclodiphosphate; HMBPP, hydroxymethylbutenyl 4-diphosphate; IPP, isopentenyl diphosphate; DMAPP, dimethylallyl diphosphate; GPP, geranyl diphosphate; GGPP, geranylgeranyl diphosphate. Enzymes are indicated in bold: DXS, DXP synthase; DXR, DXP reductoisomerase; MCT, MEP cytidylyltransferase; CMK, CDP-ME kinase; MCS, ME-cPP synthase; HDS, HMBPP synthase; HDR, HMBPP reductase; IDI, IPP isomerase; GPPS, GPP synthase; GGPPS, GGPP synthase.

Subsequently, the suspension cells were harvested for RNA isolation. The total RNA was isolated using the cetyltrimethylammonium bromide (CTAB) method[16].

2.3. Cloning of TwHDR full-length cDNA

Total RNA was reverse transcribed into first-stand cDNA with PrimeScript 1st Strand cDNA Synthesis Kit (Takara Biotechnology (Dalian) Co., Ltd., Dalian, China) due to the manufacturer's instruction. The full-length primers were designed based on the transcriptome sequencing data of *T. wilfordii* obtained previously. The prime pairs were as follow: *TwHDR*-F 5′-CTGTTCCACGCATTTTTCAACACAG-3′ and *TwHDR*-R 5′-GAGCCTAGAG GTAAAAACTGCGGTC-3′. The product was purified and cloned into the pMD19-T vector (Takara Biotechnology (Dalian) Co., Ltd., Dalian, China). The vector was transformed into *E. coli* DH5*α* cells and cultured in Luria–Bertani (LB) medium at 37 °C in dark. The positive colonies were sequenced and assembled to verify the correct *TwHDR* insertion.

2.4. Sequence alignment of HDR/IspH proteins

The nucleotide sequence was analyzed using Basic Local Alignment Search Tool (BLAST) on the National Center for Biotechnology Information (NCBI) website. The ORF and amino acid sequence of TwHDR was deduced using the ORF finder. HDR/IspH amino acid sequences from *T. wilfordii*, *Aquilaria sinensi* (AHE93332.1), *Arabidopsis thaliana* (AAN87171.1), *Salvia miltiorrhiza* (AFQ95412.1), *Nicotiana tabacum* (AAD55762.2), *Camptotheca acuminate* (ABI64152.1), *Hevea brasiliensis* (BAF98297.1), *Synechocystis* (WP_010873388.1), *Rhodobacter*

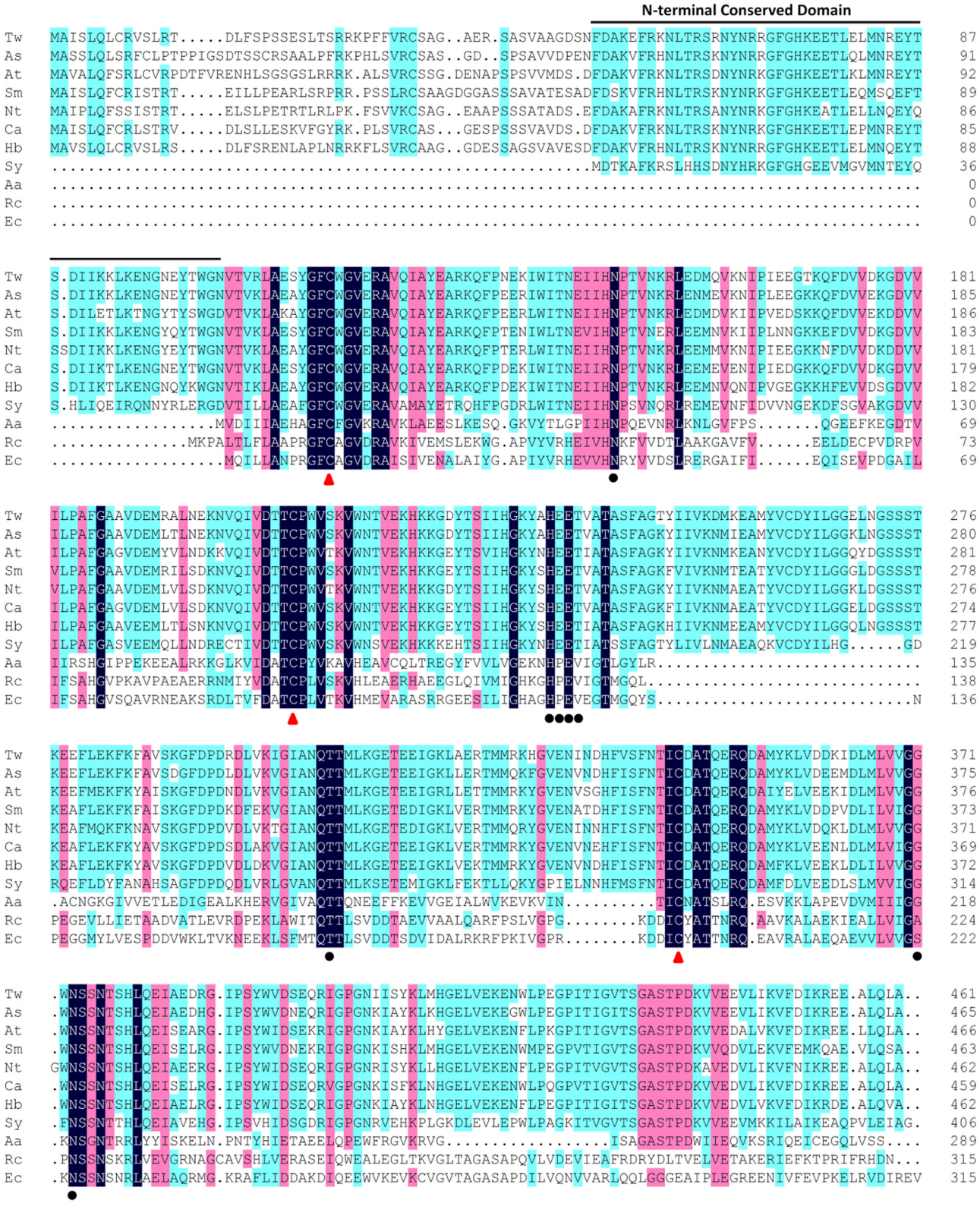

Figure 2 Amino acid sequence alignment of TwHDR with other plant HDRs and bacterial IspHs. Tw, *Tripterygium wilfordii*; As, *Aquilaria sinensi*; At, *Arabidopsis thaliana*; Sm, *Salvia miltiorrhiza*; Nt, *Nicotiana tabacum*; Ca, *Camptotheca acuminate*; Hb, *Hevea brasiliensis*; Sy, *Synechocystis* sp. PCC 6803; Aa, *Aquifex aeolicus*; Rc, *Rhodobacter capsulatus*; Ec, *Escherichia coli*. The NCD among the plants and cyanobacteria is indicated at the top of the alignment. Arrowheads indicate the critical Cys residues that are involved in iron-sulfur cluster formation. Round dots indicate the conserved amino acids near the substrate-binding site.

Capsulatus (ADE87147), *Aquifex aeolicus* (O67625), and *E. coli* (NP_414570) were aligned with Clustal Omega (http://www.ebi.ac.uk/Tools/msa/clustalo/) and DNAMAN Version 9 (Fig. 2).

2.5. Phylogenetic analysis and homology modeling of Arabidopsis HDR

TwHDR and other HDRs downloaded from GenBank were aligned, and the phylogenetic tree was constructed by the neighbor-joining method using MEGA 7.0. The 3-dimensional (3D) structural modeling was predicted by Swiss-Model.

2.6. Functional expression of TwHDR in E. coli hdr mutant

The *E. coli hdr* mutant was maintained on LB medium containing 50 μg/mL kanamycin (Kan) and 0.2% (*w/v*) arabinose (Ara)[17]. Primers 5′-CCTTGGATCCATGGCGATATCTC-3′ and 5′-CCTTGGTAC-CTTACGCTAATTGCAAG-3′ were used to amplify the full-length cDNA of *TwHDR* by PCR. The PCR products were digested with *Bam*HI and *Kpn*I, and ligated to the pQE-30 expression vector (Qiagen, Valencia, CA, USA) which was cut by the same restriction enzymes. The resulting construct pQE-*TwHDR* was transformed into *E. coli hdr* mutant competent cells and selected on LB plates containing 50 μg/mL Kan, 50 μg/mL ampicillin (Amp), and 0.2% (*w/v*) Ara. The presence of pQE-*TwHDR* plasmid in surviving colonies was verified. Transformants containing pQE-*TwHDR* plasmids were grown on LB plates containing 50 μg/mL Kan, 50 μg/mL Amp, 0.2% (*w/v*) glucose (Glc) and 0.5 mmol/L IPTG to test if the TwHDR protein could complement the *E. coli hdr* mutant. As a control, the empty pQE-30 vector was transformed into the *E. coli hdr* mutant and selected on LB plates containing 50 μg/mL Kan, 50 μg/mL Amp and 0.2% Ara.

2.7. Quantitative real-time PCR

Total RNA was used to synthesize the first strand cDNA with TIANScript II RT Kit (Tiangen Biotech (Beijing) Co., Ltd., Beijing, China), according to the manufacturer's protocols. The relative mRNA levels were estimated with the Applied Biosystems 7500 Real Time PCR System (Applied Biosystems, Grand Island, NY, USA) using KAPA SYBR® FAST qPCR Kit (KAPA Biosystems, Wilmington, MA, USA), and gene expression was quantified with the comparative C_T method (also known as the $2^{-\Delta\Delta CT}$ method). There were three samples in each group and each sample was repeated for three times to insure the credibility of the data. The real-time PCR primers were designed by Primer Premier 5.0 as follows: *β*-actin-F 5′-AGGAACCACCGATCCAGACA-3′, *β*-actin-R 5′-GGTGCCCTGAGGTCCTGTT-3′, *TwHDR* qF 5′-AATGTTACTG-TGAGACTGGCGG-3′ and *TwHDR* qR 5′-GTTGGATTGTGTAT-GATTTCGTTGG-3'.

3. Results

3.1. Cloning of full-length cDNA of TwHDR and sequence analysis of TwHDR from T. wilfordii

The full-length cDNA of *TwHDR* is 1456 bp containing a 1386 bp ORF (GenBank Accession No. KJ933412.1). The gene encodes a 461-amino-acid protein with a molecular weight of 52.1 kDa and a theoretical isoelectric point of 5.60.

BLAST result indicated that TwHDR has high homology with many plant HDRs, such as *Aquilaria sinensis* HDR (AsHDR, 85%), *Camptotheca acuminata* HDR (CaHDR, 83%), *H. brasiliensis* HDR (HbHDR, 82%), *S. miltiorrhiza* HDR (SmHDR, 78%) and *A. thaliana* HDR (AtHDR, 77%). According to the functional

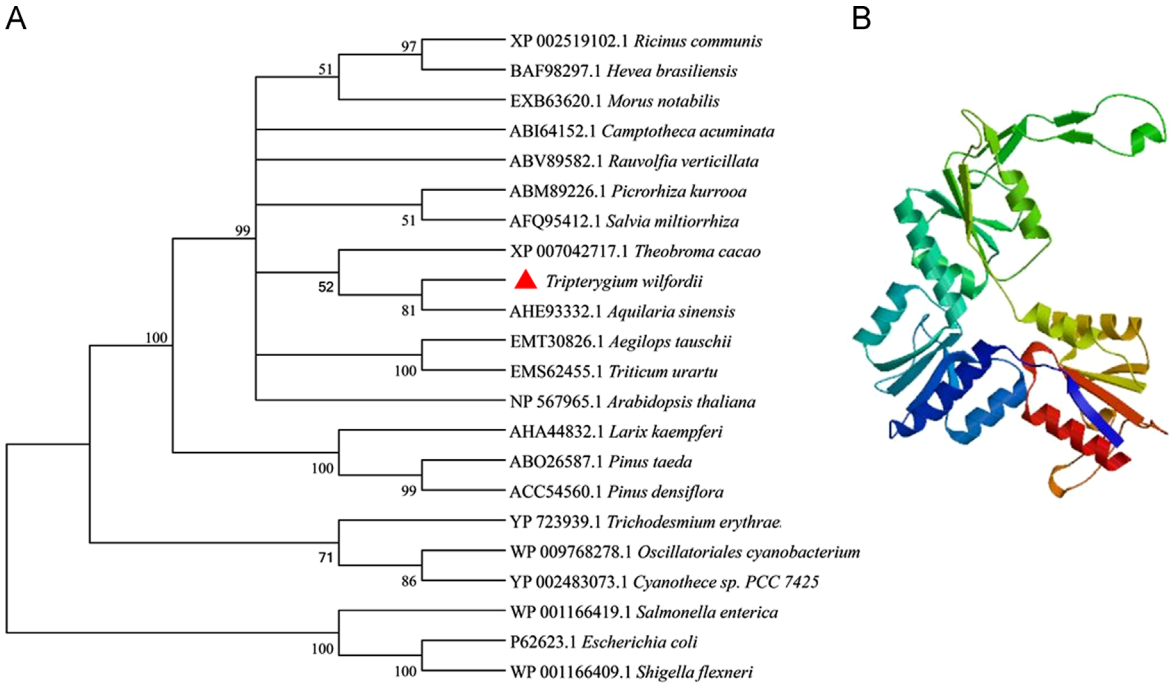

Figure 3 Phylogenetic tree analysis of the putative TwHDR and other HDRs constructed by the neighbor-joining method (A) and the 3D structure of TwHDR (B).

domain analysis, TwHDR has the IspH/LYTb domain. The sequence alignment showed that all of *E. coli*, *A. aeolicus* and *Rhodobacter capsulatus* IspHs lacked of a stretch of 53 amino acids in the N-terminus to the cyanobacterial HDR (Fig. 2). And these amino acids are highly conserved in cyanobacteria, *T. wilfordii* and other plants. And beyond the N-terminal conserved domain (NCD), the plant HDR had an extended N-terminal sequence, which was not highly conserved, and it may serve as transit peptides to target plant HDRs.

The *T. wilfordii* IspH domain (amino acid residues 106–461, encompassing the bacterial IspH) shares approximately 21.67% identity with the *E. coli* protein. Many amino acid residues found to be critical for *E. coli* and *A. aeolicus* IspHs[18–22] were also conserved in cyanobacteria and plants including *T. wilfordii*, which may play important roles as iron-sulfur cluster formation and substrate binding. Three conserved cysteine residues of the conserved residues found in TwHDR are present in all HDRs, which might participate in the coordination of the iron-sulfur bridge which might be involved in the catalysis[23] (Fig. 2). And these three cysteine residues have been proved by *E. coli* complementation assays that they are essential for *Arabidopsis* HDR function[24].

3.2. *Phylogenetic analysis and homology modeling for TwHDR*

The phylogenetic tree was constructed according to the deduced amino acid sequences of TwHDR and other HDRs from different hosts (Fig. 3A). The tree revealed that TwHDR exhibited the highest homology with HDR from *A. sinensis*. All the HDRs selected from the plants clustered together, and the HDRs from eumycophyta clustered together as another sub-branch. The HDRs from bacteria *Salmonella enterica*, *E. coli* and *Shigella flexneri* clustered as a different branch from the branch of plants and eumycophyta. 3D modeling of TwHDR was built by the Swiss-Model used the amino acids 102–453 (template: 3dnfB, Seq identity: 29.96%, Fig. 3B).

3.3. *T. wilfordii HDR complements the E. coli hdr mutant*

To further test whether the *T. wilfordii* and *E. coli* HDR proteins are functionally conserved, we performed a complementation assay with a lethal *E. coli* mutant detective in the *HDR* gene (strain MG1655). In *E. coli ispH* mutant strain MG1655 *ara* < > *ispH*, the endogenous *ispH* gene was replaced by a kanamycin-resistant cassette and a single copy of *ispH* was present on the chromosome under the control of the P_{BAD} promoter[17]. Since *HDR* gene is essential for survival, the *E. coli hdr* mutant could only grow in the medium containing Ara but not in the medium containing Glc (Fig. 4, left). Upon transformation with the constructed vector harboring the *TwHDR* gene (*pQE-TwHDR*), the lethal phenotype of the mutant strain was rescued and cells could grow in medium with Glc. The opposite was observed for cells transformed with the empty pQE-30 vector (Fig. 4 right). Therefore, the enzymatic mechanism involved in the synthesis of the isoprenoid precursors between TwHDR and *E. coli* HDR might be similar.

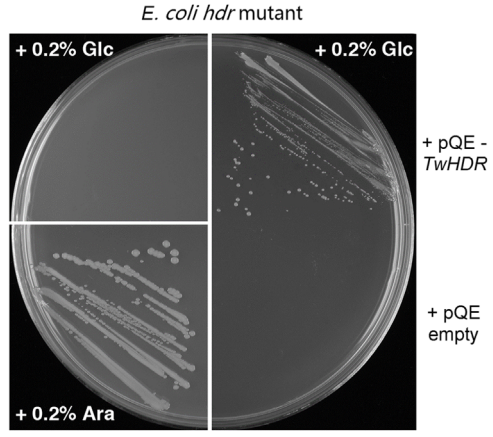

Figure 4 Complementation of *E. coli hdr* mutant strain MG1655 ara < > HDR.

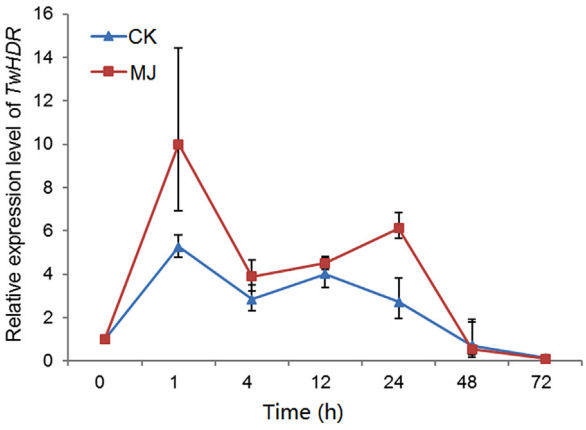

Figure 5 Expression level of *TwHDR* in suspension cells after methyl-jasmonate (MJ) treatment. CK, the control group; MJ, the MJ-induced group.

3.4. *Expression of TwHDR in the suspension cells*

As shown in Fig. 5, quantitative real-time PCR revealed the *TwHDR* expression which was induced by 50 μmol/L MJ in suspension cell cultures. The relative expression level of *TwHDR* in the MJ-induced group peaked at 1 h after the MeJA treatment (9.98 fold of that at the beginning time). After 1 h, the expression level decreased to 3.89 fold at 4 h than at 0 h. From 4 to 24 h, the expression level gradually increased, and it reached up to 6.11 fold at 24 h. And after 24 h it fell down to 10% at 72 h of that at 0 h. At the same time, in the control group, the expression level of *TwHDR* also reached its peak at 1 h. And then it progressively decreased to 13% at 72 h of that at 0 h with only a small increase between 4 and 12 h.

4. Discussion

HDR enzyme catalyzes the last step in IPP biosynthesis, playing a key role in terpenoid biosynthesis. Although *HDR* gene has been cloned from many plants, such as *A. thaliana*[25], *Ginkgo biloba*[26] and *Salvia miltiorrhizae* Bge. G. alba[27], there is no report on cloning and characterization of the *T. wilfordii* gene encoding HDR. In this study, we examined the biosynthesis pathway of terpenoid in *T. wilfordii* by cloning the *HDR* gene for the first time. *TwHDR* was transformed into a proper *E. coli* mutant strain to verify its function. Furthermore, we also examined the effects of MJ on the expression of *TwHDR*.

Although TwHDR only shares about 21.67% identity with the *E. coli* protein, it was still able to rescue the lethal phenotype of the *E. coli hdr* mutant (as shown in Fig. 4). The *E. coli* IspH protein is a reductase that possesses a dioxygen-sensitive [4Fe-4S] cluster[23]. The result of amino acid sequence alignment has demonstrated that three conserved cysteine residues which may be involved in iron-sulfur cluster formation were conserved in *E. coli* and all plant HDRs including TwHDR (Fig. 2). These results indicate that TwHDR might participate in the coordination of the iron-sulfur bridge. This complementation assay demonstrated that *TwHDR* encodes an active HDR enzyme, with similar enzymatic mechanism in the biosynthesis of IPP and DMAPP.

The expression of *TwHDR* in suspension cells was examined after 1, 4, 12, 24, 48 and 72 h of MJ treatment. The relative expression of *TwHDR* peaked at 1 h. This result indicated that a short-term MJ excitation could activate secondary metabolism MEP pathway and stimulate the plant stress defense system. About the small increase of *TwHDR* expression level between 12 and 24 h, we still cannot find the exact reason. But in the study of wound to jasmonates content in *A. sinensis*, we found the same trend[28]. In that study, the jasmonates peaked at 1 h and then decreased, after 6 h, it increased again and went to the second highest content at 24 h, and then fell again. We speculate that this variation trend may be one way that plant cultures make response to the elicitation, but more study is needed to explain its mechanism. Our results prove that TwHDR is an important enzyme in terpenoid biosynthesis pathway, which may be a good target for engineering active terpenoids in *T. wilfordii*.

Co-expression of a HDR from tomato and a taxadiene synthase from *Taxus baccata* in transgenic *A. thaliana* led to a 13-fold increase in the amount of taxadiene produced[15]. Therefore, it will be an interesting and effective way to improve triptolide content by genetic engineering. The cloning and identification of key enzyme genes in the biosynthesis of active compounds from medicinal plants is important for the analysis of synthesis pathways. Now, more and more enzyme genes in triptolide biosynthesis pathway have been cloned and identified, such as *TwDXS*[29], *TwDXR*[29], *TwFPS*[30], *TwHMGS*[31] and *TwGGPPS*[32]. Our work about cloning and identification of *TwHDR* helps know more about the biosynthesis pathway of terpenoids in *T. wilfordii*. As the biosynthesis pathway of triptolide is still unknown and the transgenic regeneration system of *T. wilfordii* remains unsolved, further studies on *HDR* and the isolation of relevant genes involved in the biosynthesis of terpenoids are still needed, which may provide insights into the production of triptolide in *T. wilfordii*.

5. Conclusions

We analyzed the function of TwHDR after successfully cloned and characterized the full-length *TwHDR* cDNA from *T. wilfordii* for the first time. The combination of cloning, identification, and functional analysis data of TwHDR will offer us more insights into the role of HDR in the MEP pathway and facilitate prospects of triptolide biosynthesis at the molecular level.

Acknowledgments

This work was supported by the National Natural Science Foundation of China (Nos. 81422053 and 81373906 to Wei Gao, and No. 81325023 to Luqi Huang) and the National High Technology Research and Development Program of China (863 Program, No. 2015AA0200908) to Wei Gao.

References

1. Tao X, Lipsky PE. The Chinese anti-inflammatory and immunosuppressive herbal remedy *Tripterygium wilfordii* Hook F. *Rheum Dis Clin North Am* 2000;**26**:29–50.
2. Han R, Rostami-Yazdi M, Gerdes S, Mrowietz U. Triptolide in the treatment of psoriasis and other immune-mediated inflammatory diseases. *Br J Clin Pharm* 2012;**74**:424–36.
3. Koo J, Arain S. Traditional Chinese medicine for the treatment of dermatologic disorders. *Arch Dermatol* 1998;**134**:1388–93.
4. Kupchan SM, Court WA, Dailey Jr RG, Gilmore CJ, Bryan RF. Triptolide and tripdiolide, novel antileukemic diterpenoid triepoxides from *Tripterygium wilfordii*. *J Am Chem Soc* 1972;**94**:7194–5.
5. Li H, Zhang YY, Huang XY, Sun YN, Jia YF, Li D. Beneficial effect of tripterine on systemic lupus erythematosus induced by active chromatin in BALB/c mice. *Eur J Pharmacol* 2005;**2**:231–7.
6. Duan H, Takaishi Y, Imakura Y, Jia Y, Li D, Cosentino LM, et al. Sesquiterpene alkaloids from *Tripterygium hypoglaucum* and *Tripterygium wilfordii*: a new class of potent anti-HIV agents. *J Nat Prod* 2000;**63**:357–61.
7. Li FQ, Lu XZ, Liang XB, Zhou HF, Xue B, Liu XY, et al. Triptolide, a Chinese herbal extract, protects dopaminergic neurons from inflammation-mediated damage through inhibition of microglial activation. *J Neuroimmunol* 2004;**148**:24–31.
8. Wang X, Liang XB, Li FQ, Zhou HF, Liu XY, Wang JJ, et al. Therapeutic strategies for Parkinson's dsease: the ancient meets the future-traditional Chinese herbal medicine, electroacupuncture, gene therapy and stem cells. *Neurochem Res* 2008;**33**:1956–63.
9. Chen YW, Lin GJ, Chia WT, Lin CK, Chuang YP, Sytwu HK. Triptolide exerts anti-tumor effect on oral cancer and KB cells *in vitro* and *in vivo*. *Oral Oncol* 2009;**45**:562–8.
10. Chappell J. Biochemistry and molecular biology of the isoprenoid biosynthetic pathway in plants. *Annu Rev Plant Physiol Plant Mol Biol* 1995;**46**:521–47.
11. Rodríguez-Concepción M, Boronat A. Breaking new ground in the regulation of the early steps of plant isoprenoid biosynthesis. *Curr Opin Plant Biol* 2015;**25**:17–22.
12. Eisenreich W, Rohdich F, Bacher A. Deoxyxylulose phosphate pathway to terpenoids. *Trends Plant Sci* 2001;**6**:78–84.
13. Lichtenthaler HK. The 1-deoxy-d-xylulose-5-phosphate pathway of isoprenoid biosynthesis in plants. *Annu Rev Plant Physiol Plant Mol Biol* 1999;**50**:47–65.
14. Page JE, Hause G, Raschke M, Gao W, Schmidt J, Zenk MH, et al. Functional analysis of the final steps of the 1-deoxy-d-xylulose 5-phosphate (DXP) pathway to isoprenoids in plants using virus-induced gene silencing. *Plant Physiol* 2004;**134**:1401–13.
15. Botella-Pavía P, Besumbes O, Phillips MA, Carretero-Paulet L, Boronat A, Rodríguez-Concepción M. Regulation of carotenoid biosynthesis in plants: evidence for a key role of hydroxymethylbutenyl diphosphate reductase in controlling the supply of plastidial isoprenoid precursors. *Plant J* 2004;**40**:188–99.
16. Del Sal G, Manfioletti G, Schneider C. The CTAB-DNA precipitation method: a common mini-scale preparation of template DNA from phagemids, phages or plasmids suitable for sequencing. *Biotechniques* 1989;**7**:514–20.
17. McAteer S, Coulson A, McLennan N, Masters M. The *lytB* gene of *Escherichia coli* is essential and specifies a product needed for isoprenoid biosynthesis. *J Bacteriol* 2001;**183**:7403–7.
18. Gräwert T, Kaiser J, Zepeck F, Laupitz R, Hecht S, Amslinger S, et al. IspH protein of *Escherichia coli*: studies on iron-sulfur cluster implementation and catalysis. *J Am Chem Soc* 2004;**126**:12847–55.
19. Gräwert T, Rohdich F, Span I, Bacher A, Eisenreich W, Eppinger J, et al. Structure of active IspH enzyme from *Escherichia coli* provides mechanistic insights into substrate reduction. *Angew Chem Int Ed Engl* 2009;**48**:5756–9.

20. Gräwert T, Span I, Eisenreich W, Rohdich F, Eppinger J, Bacher A, et al. Probing the reaction mechanism of IspH protein by X-ray structure analysis. *Proc Natl Acad Sci U S A* 2010;**107**:1077–81.
21. Rekittke I, Wiesner J, Röhrich R, Demmer U, Warkentin E, Xu W, et al. Structure of (*E*)-4-hydroxy-3-methyl-but-2-enyl diphosphate reductase, the terminal enzyme of the non-mevalonate pathway. *J Am Chem Soc* 2008;**130**:17206–7.
22. Wang W, Wang K, Liu YL, No JH, Li J, Nilges MJ, et al. Bioorganometallic mechanism of action, and inhibition, of IspH. *Proc Natl Acad Sci U S A* 2010;**107**:4522–7.
23. Wolff M, Seemann M, Bui BT, Frapart Y, Tritsch D, Estrabot AG, et al. Isoprenoid biosynthesis *via* the methylerythritol phosphate pathway: the (*E*)-4-hydroxy-3-methylbut-2-enyl diphosphate reductase (LytB/IspH) from *Escherichia coli* is a [4Fe-4S] protein. *FEBS Lett* 2003;**541**:115–20.
24. Hsieh WY, Sung TY, Wang HT, Hsieh MH. Functional evidence for the critical amino-terminal conserved domain and key amino acids of arabidopsis 4-hydroxy-3-methylbut-2-enyl diphosphate reductase. *Plant Physiol* 2014;**166**:57–69.
25. Seemann M, Wegner P, Schünemann V, Bui BT, Wolff M, Marquet A, et al. Isoprenoid biosynthesis in chloroplasts *via* the methylerythritol phosphate pathway: the (*E*)-4-hydroxy-3-methylbut-2-enyl diphosphate synthase (GcpE) from *Arabidopsis thaliana* is a [4Fe-4S] protein. *J Biol Inorg Chem* 2005;**10**:131–7.
26. Lu J, Wu W, Cao S, Zhao H, Zeng H, Lin L, et al. Molecular cloning and characterization of 1-hydroxy-2-methyl-2-(*E*)-butenyl-4-diphosphate reductase gene from *Ginkgo biloba*. *Mol Biol Rep* 2008;**35**:413–20.
27. Hao G, Shi R, Tao R, Fang Q, Jiang X, Ji H, et al. Cloning, molecular characterization and functional analysis of 1-hydroxy-2-methyl-2-(*E*)-butenyl-4-diphosphate reductase (*HDR*) gene for diterpenoid tanshinone biosynthesis in *Salvia miltiorrhiza* Bge. f. alba. *Plant Physiol Biochem* 2013;**70**:21–32.
28. Zhang Z, Yang Y, Wei JH, Meng H, Wang MX, Han XM, et al. Response of endogenous jasmonates and sesquiterpenes to mechanical wound in *Aquilaria sinensis* stem. *Acta Hortic Sin* 2013;**40**:163–8.
29. Tong Y, Su P, Zhao Y, Zhang M, Wang X, Liu Y, et al. Molecular cloning and characterization of *DXS* and *DXR* genes in the terpenoid biosynthetic pathway of *Tripterygium wilfordii*. *Int J Mol Sci* 2015;**16**:25516–35.
30. Zhao YJ, Chen X, Zhang M, Su P, Liu YJ, Tong YR, et al. Molecular cloning and characterisation of farnesyl pyrophosphate synthase from *Tripterygium wilfordii*. *PLoS One* 2015;**10**:e0125415.
31. Liu YJ, Zhao YJ, Zhang M, Su P, Wang XJ, Zhang XN, et al. Cloning and characterisation of the gene encoding 3-hydroxy-3-methylglutaryl-CoA synthase in *Tripterygium wilfordii*. *Molecules* 2014;**19**:19696–707.
32. Zhang M, Su P, Zhou YJ, Wang XJ, Zhao YJ, Liu YJ, et al. Identification of geranylgeranyl diphosphate synthase genes from *Tripterygium wilfordii*. *Plant Cell Rep* 2015;**34**:2179–88.